Received: 11 May 2020 | Revised: 24 June 2020 | Accepted: 15 July 2020

DOI: 10.1002/hbm.25155

RESEARCH ARTICLE

WILEY

Unsupervised clustering of dopamine transporter PET imaging discovers heterogeneity of parkinsonism

Minseok Suh[1,2] | Jin Hee Im[3] | Hongyoon Choi[1] | Han-Joon Kim[3] | Gi Jeong Cheon[1] | Beomseok Jeon[3]

[1]Department of Nuclear Medicine, Seoul National University Hospital, Seoul, South Korea

[2]Department of Molecular Medicine and Biopharmaceutical Sciences, Graduate School of Convergence Science and Technology, Seoul National University, Seoul, South Korea

[3]Department of Neurology and Movement Disorder Center, Seoul National University Hospital, Seoul, South Korea

Correspondence
Hongyoon Choi, Department of Nuclear Medicine, Seoul National University Hospital, 101 Daehak-ro, Jongno-gu, Seoul 03080, South Korea.
Email: chy1000@snu.ac.kr

Han-Joon Kim, Department of Neurology, Seoul National University Hospital, 101 Daehak-ro, Jongno-gu, Seoul 03080, South Korea.
Email: movement@snu.ac.kr

Funding information
National Research Foundation of Korea, Grant/Award Numbers: NRF-2019K1A3A1A14065446, NRF-2019R1F1A1061412

Abstract

Parkinsonism has heterogeneous nature, showing distinctive patterns of disease progression and prognosis. We aimed to find clusters of parkinsonism based on ^{18}F-fluoropropyl-carbomethoxyiodophenylnortropane (FP-CIT) PET as a data-driven approach to evaluate heterogenous dopaminergic neurodegeneration patterns. Two different cohorts of patients who received FP-CIT PET were collected. A labeled cohort (n = 94) included patients with parkinsonism who underwent a clinical follow-up of at least 3 years (mean 59.0 ± 14.6 months). An unlabeled cohort (n = 813) included all FP-CIT PET data of a single-center. All PET data were clustered by a dimension reduction method followed by hierarchical clustering. Four distinct clusters were defined according to the imaging patterns. When the diagnosis of the labeled cohort of 94 patients was compared with the corresponding cluster, parkinsonism patients were mostly included in two clusters, cluster "0" and "2." Specifically, patients with progressive supranuclear palsy were significantly more included in cluster 0. The two distinct clusters showed significantly different clinical features. Furthermore, even in PD patients, two clusters showed a trend of different clinical features. We found distinctive clusters of parkinsonism based on FP-CIT PET-derived heterogeneous neurodegeneration patterns, which were associated with different clinical features. Our results support a biological underpinning for the heterogeneity of neurodegeneration in parkinsonism.

KEYWORDS

^{18}F-FP-CIT PET, clustering, Parkinson's disease, parkinsonism, unsupervised learning

1 | INTRODUCTION

Parkinsonism is a clinical syndrome with distinctive disease entities, including idiopathic Parkinson's disease, multiple system atrophy (MSA) and progressive supranuclear palsy (PSP). By sharing dopaminergic neurodegeneration in common, parkinsonism can be characterized by a combination of clinical features such as bradykinesia, rigidity, resting tremor, and postural instability (Hughes, Daniel, & Lees, 1993; Jankovic, 2008). Despite considerable common motor symptoms, clinical presentations and prognosis of parkinsonism are heterogeneous among each of disease entities (Aleksovski, Miljkovic, Bravi, & Antonini, 2018; Fereshtehnejad et al., 2015; Foltynie, Brayne, & Barker, 2002; Marras &

Chaudhuri, 2016; Marras & Lang, 2013; Thenganatt & Jankovic, 2014; Titova, Padmakumar, Lewis, & Chaudhuri, 2017; van Rooden et al., 2011). Because of broad clinical overlap, an objective and reproducible biomarker based on the neurodegeneration pattern is needed to better understand the disease progression and to predict patient's prognosis in a personalized manner, which may eventually aid establishing efficient treatment strategies of parkinsonism (Espay et al., 2017; Tolosa, Wenning, & Poewe, 2006).

The dopamine transporter (DAT) is known to be the single most important factor of extracellular dopamine concentration, reflecting the axonal dysfunction (Nutt, Carter, & Sexton, 2004; Saari et al., 2017). DAT imaging does not directly reflect dopaminergic neurons, but still, as from the previous study, showing a positive correlation of DAT binding and symptom duration, it reflects the dopaminergic neuronal functionality (Saari et al., 2017). Furthermore, the loss of dopaminergic function is associated with phenotypic changes in the nigrostriatal systems and affects clinical presentation in the early disease state (Kordower et al., 2013). DAT imaging using SPECT (Single-photon emission computed tomography) or positron emission tomography (PET) is a well-established method for evaluating dopaminergic neurodegeneration. Thus, it has now been widely used due to the clinical utility in the diagnosis of parkinsonism (Catafau, Tolosa, & Da, 2004). In particular, ^{18}F-fluoropropyl-carbomethoxyiodophenylnortropane (FP-CIT) PET has a relatively higher resolution than SPECT, which enables us to find spatial patterns of neurodegeneration of parkinsonism(Lee et al., 2018; Oh et al., 2012). Accordingly, the heterogeneity of parkinsonism in terms of dopaminergic dysfunction and its related clinical presentation may be associated with the spatial degeneration patterns identified by FP-CIT PET.

In this study, we aimed to identify the heterogeneity of parkinsonism in terms of the spatial patterns of dopaminergic neurodegeneration. As a data-driven approach, a large dataset of FP-CIT PET was used to capture spatial patterns of FP-CIT PET and to find clusters. Since this approach is a type of work discovering different groups using only imaging patterns without clinical diagnostic labels, it is possible to propose a robust and reproducible parkinsonism cluster, which is expected to eventually be used as an imaging biomarker to objectively evaluate parkinsonism (Choi, Jin, & Initiative, 2018).

2 | MATERIALS AND METHODS

2.1 | Subjects

Two different cohorts were included for this study: labeled and unlabeled cohorts. The labeled cohort consists of 94 patients with parkinsonism who underwent FP-CIT PET in the early stage of the disease and then followed for at least 3 years (mean 59.0 ± 14.6 months) when a diagnostic re-appraisal was made. Diagnosis of PD, MSA-P (parkinsonian type), and PSP was made according to the clinical diagnostic criteria and all patients were assessed by neurologists specialized in movement disorders (Gilman et al., 2008; Hughes, Daniel, Kilford, & Lees, 1992; Litvan et al., 1996). Among these 94 patients, 49 patients were idiopathic Parkinson's disease, 17 patients were MSA-P and 10 patients were PSP. Sixteen patients had parkinsonism with uncertain diagnosis even at re-appraisal. One patient was found not to have parkinsonism through follow-up. Corresponding clinical features such as autonomic nerve symptom (ANS), cognitive deficit, dyskinesia, and freezing of gait (FOG) were assessed at the time of the last diagnosis. All patients underwent FP-CIT PET at baseline for differentiating parkinsonism, the mean period between motor symptom onset and FP-CIT PET was 1.98 ± 1.87 years. FP-CIT PET studies were acquired from July 2009 to Sep 2013.

Another cohort, the unlabeled cohort (n = 813), included all FP-CIT PET data acquired from Jan 2015 to June 2018. This cohort included all FP-CIT PET data acquired in a single-center, which were acquired for evaluating patients with parkinsonism and other neurodegenerative disorders.

This study was approved by the Institutional Review Board of our institute, and informed consent was waived as a retrospective design. All procedures performed in this study were under the ethical standards of the institutional research committee and with the 1964 Helsinki declaration and its later amendments or comparable ethical standards.

2.2 | FP-CIT PET/CT acquisition

As a clinical routine protocol, patients underwent PET/CT imaging, 2 hr after 185 MBq (5 mCi) of ^{18}F-FP-CIT injection. Emission scans were acquired for 10 min using dedicated PET/CT scanners (Biograph 40 or mCT, Siemens, Erlangen, Germany), followed by CT scans for attenuation correction. PET images were reconstructed by an iterative algorithm (ordered-subset expectation maximization, OSEM) with 24 subsets and 5 iterations. Images were reconstructed with the same matrix size with 256×256. Four millimeters of Gaussian post-reconstruction filter was applied.

2.3 | Image preprocessing and calculation of binding ratio

All the PET images were spatially normalized into an in-house ^{18}F-FP-CIT PET template (Choi et al., 2016; Kim et al., 2012). The spatial normalization was performed using statistical parametric mapping software (SPM8, University College of London, London, UK). Voxel counts were changed to binding ratio, defined as $BR = C_{specific}/C_{nonspecific}$, where C represented PET counts. Mean counts of occipital cortex were regarded as nonspecific binding, $C_{nonspecific}$. Automated Anatomical Labeling (AAL) was used for predefined volume-of-interests to define the occipital cortex as well as the striatum. The voxel size of spatially normalized BR maps was $2.0 \times 2.0 \times 2.0$ mm. The binding ratio of the putamen and caudate was obtained by the predefined AAL VOIs. BR of bilateral putamen and caudate were calculated by the volume-of-interests and mean values were used. We also included qualitative evaluation of FP-CIT PET of all data using

the formal reading reports. All reports of all FP-CIT PET was made by a consensus of more than two nuclear medicine brain imaging experts. We classified all FP-CIT PET images into two classes of whether imaging patterns suggested dopaminergic neurodegeneration or not.

2.4 | Unsupervised clustering of FP-CIT PET data

All FP-CIT PET data (n = 907) were clustered according to the brain BR of FP-CIT patterns. Firstly, principal component analyses (PCA) were applied for data dimension reduction. PCA determines a set of linearly uncorrelated features that account for variability in a dataset. All spatially normalized FP-CIT PET data were changed to a matrix $M_{i,j}$, where i is the number of subjects and j is the number of voxels of the brain. Principal components (PCs) were computed from the SVD (singular value decomposition) of the matrix. The matrix was centered by subtracting the mean image and then decomposed to n components: $M = USV^T$. PCs are given by SV^T and the contribution of the kth PC to the ith subject is given by the $U(i,k)$. We extracted 10 PCs from FP-CIT PET data.

Samples were clustered by a hierarchical clustering method. Using PCs of all FP-CIT PET data, the similarity was determined by the average distance between elements of each hierarchical cluster. A given cutoff of the hierarchical dendrogram provides a number of clusters, resulting in four clusters that reflect FP-CIT PET patterns.

2.5 | Data visualization by 2-dimensional projection

To intuitively visualize FP-CIT PET patterns, another dimension reduction method, t-distributed stochastic neighborhood embedding (t-SNE), was employed (Maaten & Hinton, 2008). t-SNE retains local similarities between data in a way that similar FP-CIT PET are modeled by nearby points and dissimilar samples are modeled by distant points. The similarity between data is modeled as Gaussian with a given number of neighbors, perplexity. Here, we set the perplexity to 30 and we reduced dimension to two axes.

2.6 | Statistics

As all data including the labeled and unlabeled cohorts were clustered by FP-CIT PET patterns, final clinical diagnosis, and clinical symptoms were compared for patients with different clusters in the labeled cohort. In particular, clinical symptoms including the freezing of gait, autonomic nerve symptoms, and dyskinesia were compared for patients with different clusters. Student's t-test was used to compare continuous variables including BR of two different clusters. The differences between groups were considered statistically significant at p-value < .05. Pearson's chi-square test was performed to analyze the categorical variables including clinical symptoms.

3 | RESULTS

3.1 | Four clusters identified from FP-CIT PET patterns

Brief demographics of labeled and unlabeled cohorts were summarized in Table 1. PCs, the sets of linearly uncorrelated image-based patterns, were extracted from all FP-CIT PET data (Figure 1a). The anatomical location of peak voxels is summarized in Table S1. Notably, these patterns were extracted from all subjects using a data-driven unsupervised manner without labels such as clinical diagnosis. Imaging patterns were divided into four clusters by hierarchical clustering. A heatmap for PCs of all cohorts and conventional BR quantification results is presented in Figure 1b. Averaged FP-CIT PET images across the patients with the same cluster was represented in Figure 1c.

All data were intuitively visualized by 2-dimensional embedding using t-SNE plots (Figure 2, Figure S1). All images were divided into visually normal and abnormal patterns according to the formal report which includes visual interpretation of FP-CIT PET (Figure 2a). By mapping with the quantification of caudate and putamen BR, Putamen and caudate BR were differently associated with data distribution patterns on the t-SNE plot (Figure 2b,c). The t-SNE map was also plotted with the four clusters (Figure 2d). The cluster 0 and cluster 2 were mostly overlapped with visually abnormal patterns and cluster 1 and cluster 3 were mostly overlapped with visually normal patterns.

3.2 | FP-CIT PET-based clusters associated with different diagnosis of parkinsonism

We then applied the clusters to the labeled cohort, which included 94 patients who were clinically diagnosed as Parkinson's disease, PSP, MSA-P, or parkinsonism with uncertain diagnosis (Figure 3a). Cluster 0 and cluster 2 showed different patterns particularly in PC1 and PC2,

TABLE 1 Demographics and clusters based on FP-CIT PET

	Labeled cohort (n = 94)	Unlabeled cohort (n = 813)
Age	61.9 ± 10.3 (range: 30.4–80.5)	67.5 ± 10.4 (range: 12.9–95.9)
Sex	M:F = 41:53	M:F = 357:456
Clusters	0–41 1–5 2–47 3–1	0–258 1–272 2–189 3–94
Diagnosis	Parkinson's disease – 49 Progressive Supranuclear palsy – 10 Multiple system atrophy (Parkinsonian type) – 17 Diffuse Lewy body disease – 1 Other parkinsonism – 16 Non-parkinsonian disorder – 1	N/A

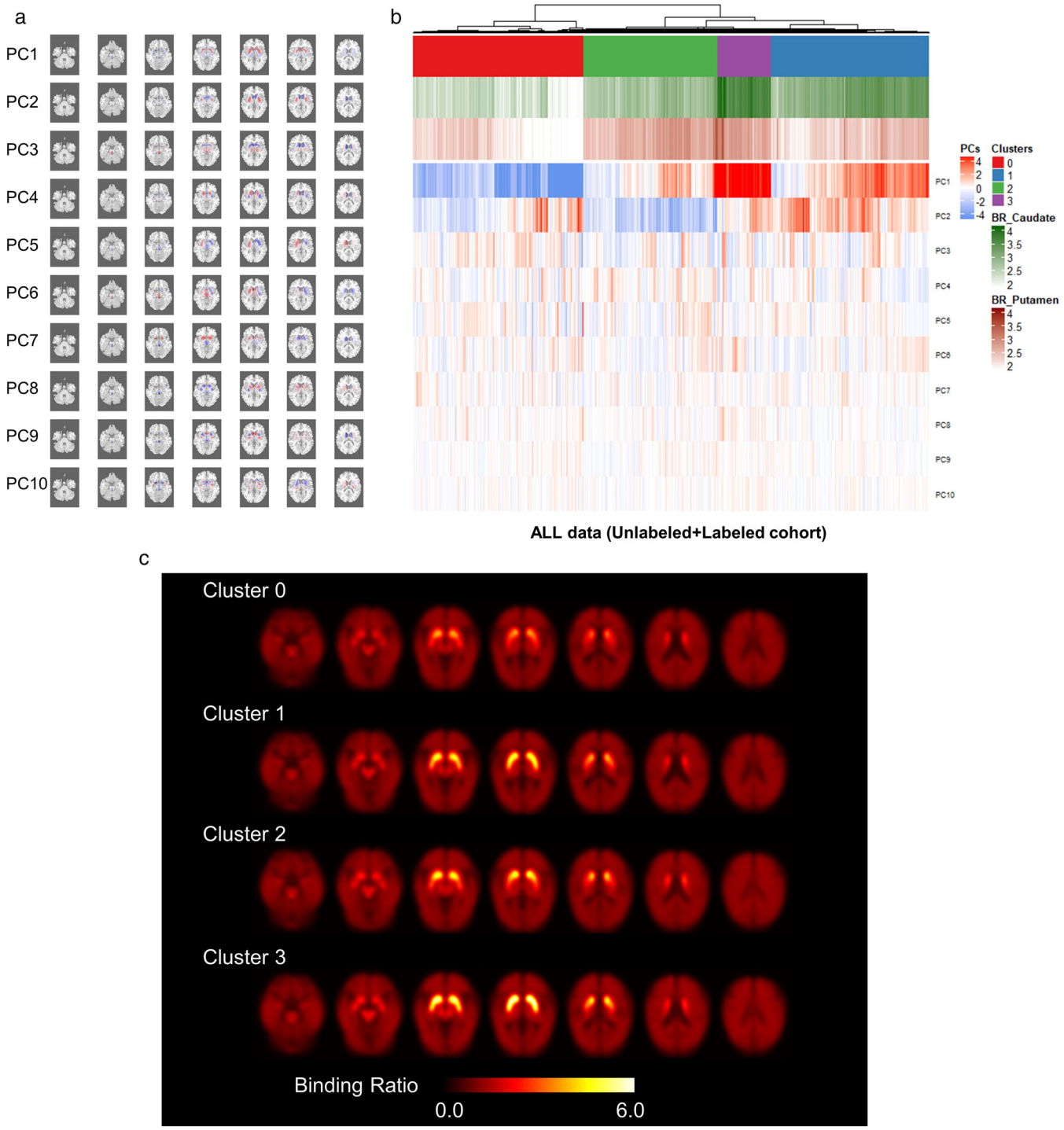

FIGURE 1 Unsupervised clustering of FP-CIT PET. (a) Spatial patterns extracted by the principal component analysis were represented. Note that red color represented positively associated voxels and blue color represented negatively associated voxels of a given principal component (PC). (b) A total of 907 FP-CIT PET images were clustered by a hierarchical clustering method using principal components. Four different clusters were identified. (c) Mean FP-CIT PET images of the four different clusters were represented

while PC3 of cluster 0 and cluster 2 were not significantly different (Figure S2). Notably, PC1 was associated with BR of the whole putamen, while PC2 was associated with BR of posterior putamen. The frequency of clinical diagnosis was significantly different according to the FP-CIT PET-based clusters (chi-square = 35.4, p = .0004) (Figure 3b,c). Among 94 patients, 88 patients with parkinsonism were classified as either cluster 0 or cluster 2. PSP was significantly more classified as the cluster 0 compared with other clusters

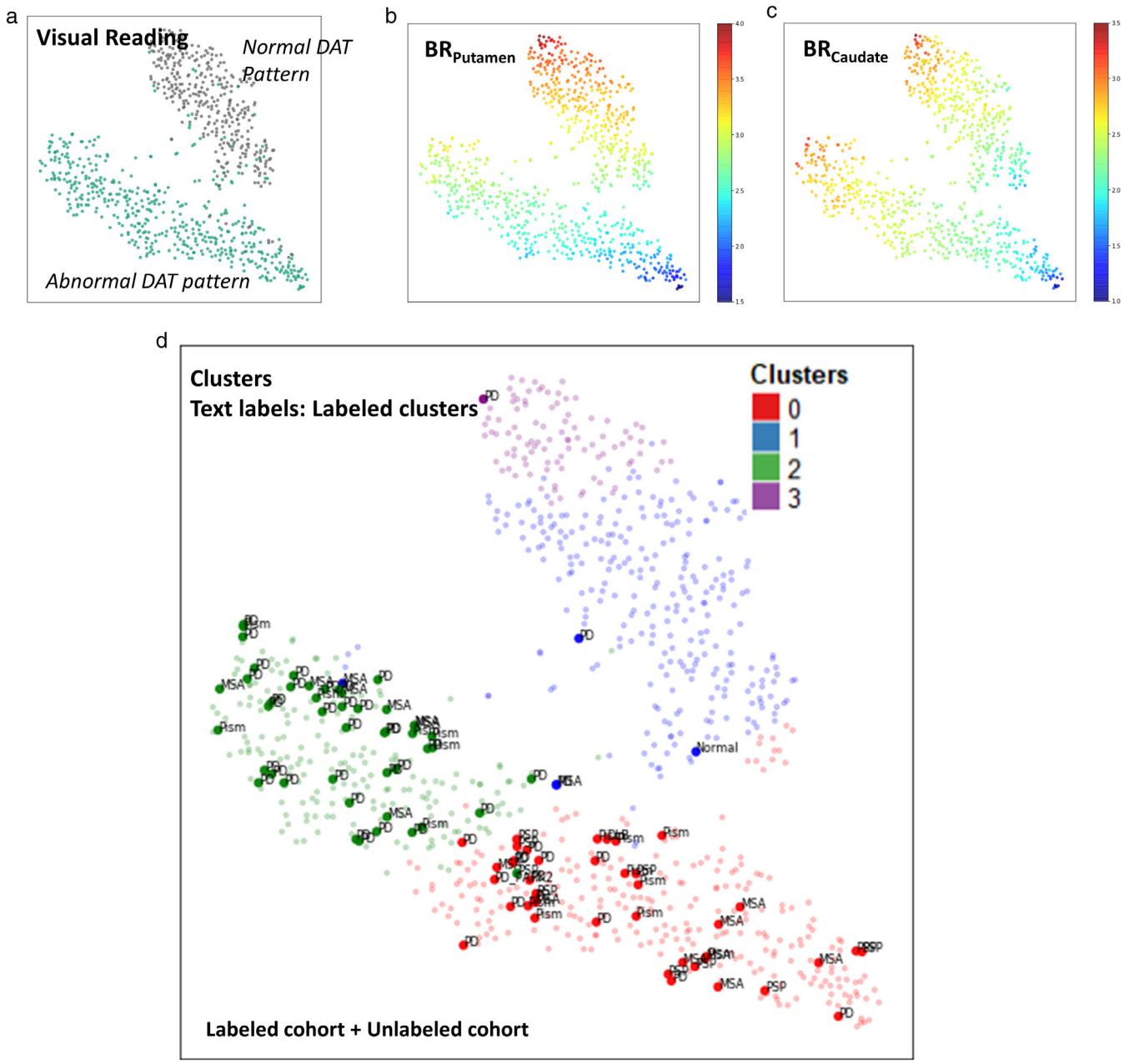

FIGURE 2 Spatial patterns of FP-CIT PET. To visualize the relationship of PET images, a 2-dimensional projection map was drawn using t-distributed stochastic neighborhood embedding (t-SNE). (a) The t-SNE map was represented with two different groups according to visual interpretation. The points of the t-SNE map were colored with conventional quantification results of FP-CIT PET, including binding ratio (BR) of the putamen (b) and caudate (c). (d) FP-CIT PET images of the labeled cohort which has diagnostic label according to clinical follow-up were represented on the t-SNE map. Colors represented the clusters estimated by the unsupervised clustering

(chi-square = 9.7, p = .002). In cluster 2, only one patient was PSP, while nine patients with PSP were classified as cluster 0 (Figure 3b). The deviation of diagnosis in different clusters were presented by an association plot (Figure 3c). The colored bar indicated more frequent diagnosis in the cluster.

Onset age and disease duration of both clusters were not significantly different (cluster 0 vs. cluster 2:60.4 ± 11.6 vs. 58.1 ± 9.0 and 2.3 ± 1.8 vs. 2.3 ± 1.7 for onset age and duration between onset to PET scan, respectively). Patients in the cluster 0 showed poor response to levodopa treatment compared with cluster 2 (73.2% and 89.3% in cluster 0 and cluster 2, respectively, p = .049). FOG (cluster 0 vs. cluster 2; 53.6% vs. 23.4%, p = .003), ANS (70.7% vs. 46.8%, p = .023) and cognitive deficit (39.0% vs. 14.9%, p = .010) were significantly more common in cluster 0 (Table 2).

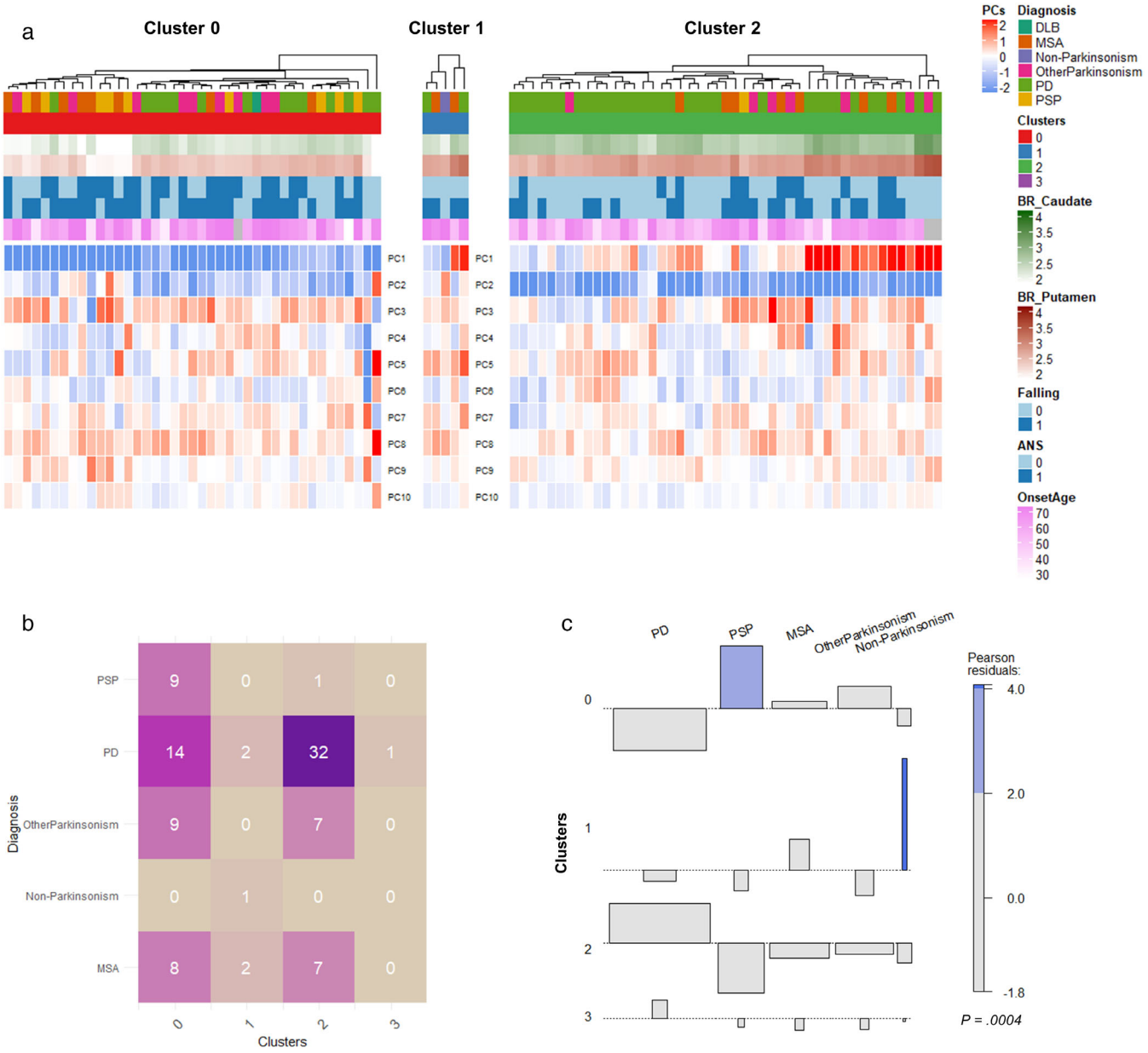

FIGURE 3 Association of FP-CIT PET-based clusters and clinical diagnosis. (a) A heatmap was drawn for the labeled cohort with diagnosis and clinical presentations. (b) The number of patients of each diagnostic label was represented with FP-CIT PET-based clusters. Most patients were included in cluster 0 and cluster 2. (c) An association plot was drawn for assessing the deviation of diagnostic labels according to the clusters. Blue color represented a positive deviation of diagnostic labels for each cluster, suggesting the high frequent diagnosis in a given cluster compared with other clusters. BR, binding ratio; MSA, multiple system atrophy; PD, Parkinson's disease; PSP, progressive supranuclear palsy

TABLE 2 Clinical features of patients with parkinsonism according to FP-CIT PET-based clusters

Features	Cluster 2 (*n* = 47)	Cluster 0 (*n* = 41)	*p*-Value
Onset age	58.1 ± 9.0	60.4 ± 11.6	N.S.
Duration (onset to scan)	2.3 ± 1.8	2.3 ± 1.7	N.S.
Symptoms			
DOPA response	42 (89.3%)	30 (73.2%)	.049
Freezing of gait	11 (23.4%)	22 (53.6%)	.003
Autonomic nerve symptoms	22 (46.8%)	29 (70.7%)	.023
Cognitive deficit	7 (14.9%)	16 (39.0%)	.010
Dyskinesia	12 (25.5%)	7 (17.1%)	N.S.

3.3 | Difference of clinical presentation in FP-CIT PET-based clusters of Parkinson's disease patient

Among 49 Parkinson's disease patients, 32 were included in the cluster 2 and 14 were included in the cluster 0. The Parkinson's disease patients with the different clusters show different patterns of clinical features as well as FP-CIT BR. Both BR of putamen and caudate were significantly lower in Parkinson's disease patients of the cluster 0 than those of the cluster 2 (2.44 ± 0.29 vs. 2.85 ± 0.21, p = .0001 for putamen; 2.33 ± 0.25 vs. 2.75 ± 0.19, p < .0001 for caudate) (Figure S3). Onset age and disease duration were not significantly different between two clusters (cluster 0 vs. cluster 2; 56.2 ± 12.6 vs. 55.4 ± 9.0 and 1.71 ± 1.38 vs. 2.16 ± 1.69 years, onset age and disease duration, respectively) (Figure S3). FOG was significantly more common in the cluster 0 (35.7% and 9.4% of Parkinson's disease patients in cluster 0 and cluster 2, respectively, p = .03). On the other hand, dyskinesia appeared more common in the Parkinson's disease patients in the cluster 2, though it did not reach a statistical significance (34.4% for the cluster 2 vs. 14.3% for the cluster 0, p = .16) (Table 3).

4 | DISCUSSION

In the present study, four distinct clusters were defined according to the spatial patterns of dopaminergic degeneration on DAT imaging. Two clusters, cluster 0 and cluster 2, mainly comprised DAT images with a visually abnormal pattern, which has been a clinically routine and conventional qualitative interpretation. When the labeled cohort, which included patients with parkinsonism according to the clinical diagnosis, was analyzed with corresponding clusters, Parkinson's disease and other atypical parkinsonism mostly occupied cluster 0 and cluster 2. These two clusters showed a different distribution of disease entities, diagnosis based on 3 years follow-up, and distinctive clinical features. Furthermore, even among patients with the diagnosis of Parkinson's disease, different clinical features were observed between two clusters. Our finding suggested the heterogeneity of parkinsonism in terms of the various dopaminergic neurodegeneration patterns.

The image patterns used for the clustering were in a similar vein with previous studies regarding different sub-regional DAT loss patterns according to each entity of parkinsonism. Kahraman et al. revealed visually distinct DAT patterns between atypical parkinsonism and idiopathic Parkinson's disease using ^{123}I-FP-CIT SPECT (Kahraman, Eggers, Schicha, Timmermann, & Schmidt, 2012). Diffuse and severe DAT loss pattern was a predictive marker for atypical parkinsonism. More recently, PSP patients show extensive and symmetric DAT loss across the whole striatum, while Parkinson's disease and MSA-P patients show relatively preserved binding in the caudate nucleus and anterior putamen (Antonini et al., 2003; Filippi et al., 2006; Oh et al., 2012). These DAT image studies were supported by the Post-mortem study revealing excessive neuronal loss in PSP compared with Parkinson's disease (Murphy, Karaconji, Hardman, & Halliday, 2008). In our results, cluster 0 mainly showed an extensive DAT loss in the whole striatum associated with PC1, and atypical parkinsonism patients, specifically PSP, were mainly included in this cluster. Cluster 2, which was more relevant to typical Parkinson's disease, showed relatively preserved DAT binding in the anterior portion of the putamen and relatively decreased DAT binding in the posterior putamen, related to reduced PC2 (Figure 1c).

The heterogeneous neurodegeneration patterns of FP-CIT PET proved its clinical implication by showing distinctive clinical presentations among the labeled cohort of parkinsonism patients. Cluster 0, which mainly represents atypical parkinsonism, showed clinical characteristics of significantly poor treatment response, high FOG, high frequency of ANS, and more cognitive deficit. Parkinson's disease patients who were allocated in the cluster 0 also showed significantly high FOG presentation, but relatively low dyskinesia. Previous subtype studies reported that, in addition to the cognitive deficit, FOG and lack of dyskinesia, which implies poor dopamine response, were relevant to Parkinson's disease subtypes defined as *diffuse/malignant* (Fereshtehnejad et al., 2015) and *Postural Instability/gait disturbance* (Aleksovski et al., 2018), and also, it is known to be a commonly observed feature of atypical parkinsonism, including PSP, MSA-P, and dementia with Lewy bodies (Giladi, Kao, & Fahn, 1997). ANS is a key configuration for Parkinson's disease subtyping and is a characteristic feature of MSA-P. These clinical features, all in common, are related to severe disease manifestation and poor prognosis, which might be the clinical characteristic of cluster 0. Poor levodopa response observed in our study further refine the characteristics of this cluster. On the other hand, although not significant, patients allocated in the cluster 2 show a high prevalence of dyskinesia, which is associated with levodopa responsiveness, and thus, favors a diagnosis of Parkinson's disease over atypical parkinsonism (Postuma et al., 2015). As future work, further in-depth investigation regarding the clinical outcome of these different two clusters in parkinsonism patients could clarify the association of heterogeneous neurodegeneration patterns and prognosis.

Recently, many attempts using cluster analysis, based on diverse clinical features, have been made to identify distinct subtypes of

TABLE 3 Clinical symptoms of patients with Parkinson's disease, a subgroup of the labeled cohort, according to FP-CIT PET-based clusters

Symptoms	Cluster 2 (n = 32)	Cluster 0 (n = 14)	p-Value
DOPA response	32 (100%)	14 (100%)	N.S.
Freezing of gait	3 (9.4%)	5 (35.7%)	.03
Autonomic nerve symptoms	12 (37.5%)	6 (42.9%)	N.S.
Cognitive deficit	2 (6.3%)	1 (7.1%)	N.S.
Dyskinesia	11 (34.4%)	2 (14.3%)	.16

Parkinson's disease (De Pablo-Fernandez, Lees, Holton, & Warner, 2019; Erro et al., 2016; Faghri et al., 2018; Fereshtehnejad et al., 2015; Lawton et al., 2018). Longitudinal follow-up studies revealed the relevance of subtype classification at an early stage with treatment response (Lawton et al., 2018), disease course, and survival (De Pablo-Fernandez et al., 2019). However, the lack of a valid and robust method for subtyping Parkinson's disease only based on clinical features has made it fail to reproduce in a clinical trial cohort (Mestre et al., 2018). More specifically, previous subtyping systems used a combination of diverse phenotypes of the disease, which was hard to be supported by a plausible explanation of the pathophysiologic process such as neurodegeneration of Parkinson's disease. Such a lack of reproducibility and consideration for pathophysiology have limited widely acceptable subtyping system in the clinic. On the other hand, our data-driven approach based on unsupervised clustering of imaging employing a relatively large dataset is robust, since there is little room for ambiguous and subjective elements to intervene. Thus, FP-CIT PET-based clustering methods could be objective and reproducible. Furthermore, as FP-CIT PET directly reflects the DAT expression and dopaminergic function (Ba & Martin, 2015; Saari et al., 2017), our approach could lead to suitable biomarker development for subtyping of Parkinson's disease by explaining the heterogeneous neurodegeneration patterns.

Some limitations should be noted. Firstly, validated motor scales, such as UPDRS (Unified Parkinson's Disease Rating Scale) for PD, UMSARS (Unified Multiple System Atrophy Rating Scale) for MSA, were not performed in the labeled cohort. Despite the absence of disease-specific symptom scales, patients were regularly examined for a sufficiently long-term period, and at every visit reevaluated to consolidate the clinical diagnosis. Secondly, as a single institute retrospective study, the number of patients with MSA-P and PSP was relatively limited. However, we speculate that, since comprehensive diagnosis was made through long term clinical assessment, each group would well reflect the disease entity. Nonetheless, prospective cohort studies with a larger number of patients and comprehensive neurological symptom evaluation will be necessary to solidify the clinical significance of our data-driven approach. Furthermore, a longitudinal follow-up study will corroborate whether the FP-CIT PET-based clusters have a clinical value to predict disease progression and outcome.

The unsupervised clustering of FP-CIT PET showed a heterogeneous pattern of dopaminergic neurodegeneration in patients with parkinsonism. These clusters were associated with different diagnosis of parkinsonism. Furthermore, the results of distinctive clinical features observed between different clusters in Parkinson's disease as well as all patients with parkinsonism, support the clinical heterogeneity of parkinsonism in terms of dopaminergic neurodegeneration. Furthermore, we expect that our approach of a quantitative assessment of degeneration patterns using PCs and FP-CIT PET PET-based clusters can be used at each patient level. Although further clinical validation studies are needed, this approach may be applied to predicting the course of clinical symptoms particularly in patients with early parkinsonism as well as Supporting Information on differential diagnosis of parkinsonism. Our data-driven approach to identify the heterogeneity will lead to a better understanding of the disease and personalized management of the patient.

CONFLICT OF INTEREST

The authors declare no potential conflict of interest.

AUTHOR CONTRIBUTIONS

Hongyoon Choi and Han-Joon Kim designed the study. Minseok Suh and Hongyoon Choi analyzed imaging data. Jin Hee Im and Han-Joon Kim collected and analyzed clinical data. Gi Jeong Cheon and Beomseok Jeon interpreted results and supported the analysis. All authors wrote and edited the manuscript. All authors approved the manuscript.

DATA AVAILABILITY STATEMENT

Our PET data with anonymized personal information will be accessible to readers upon reasonable request and following the completion of our ongoing projects.

ETHICS STATEMENT

This study was approved by the Institutional Review Board of our institute, and informed consent was waived as a retrospective design. All procedures performed in this study were in accordance with the ethical standards of the institutional research committee and with the 1964 Helsinki declaration and its later amendments or comparable ethical standards.

ORCID

Hongyoon Choi https://orcid.org/0000-0002-8895-2449

REFERENCES

Aleksovski, D., Miljkovic, D., Bravi, D., & Antonini, A. (2018). Disease progression in Parkinson subtypes: The PPMI dataset. *Neurological Sciences*, *39*(11), 1971–1976. https://doi.org/10.1007/s10072-018-3522-z

Antonini, A., Benti, R., De Notaris, R., Tesei, S., Zecchinelli, A., Sacilotto, G., … Gerundini, P. (2003). 123I-Ioflupane/SPECT binding to striatal dopamine transporter (DAT) uptake in patients with Parkinson's disease, multiple system atrophy, and progressive supranuclear palsy. *Neurological Sciences*, *24*(3), 149–150. https://doi.org/10.1007/s10072-003-0103-5

Ba, F., & Martin, W. R. (2015). Dopamine transporter imaging as a diagnostic tool for parkinsonism and related disorders in clinical practice. *Parkinsonism & Related Disorders*, *21*(2), 87–94. https://doi.org/10.1016/j.parkreldis.2014.11.007

Catafau, A. M., Tolosa, E., & Da, T. C. U. P. S. S. G. (2004). Impact of dopamine transporter SPECT using 123I-Ioflupane on diagnosis and management of patients with clinically uncertain Parkinsonian syndromes. *Movement Disorders*, *19*(10), 1175–1182. https://doi.org/10.1002/mds.20112

Choi, H., Cheon, G. J., Kim, H. J., Choi, S. H., Kim, Y. I., Kang, K. W., … Lee, D. S. (2016). Gray matter correlates of dopaminergic degeneration in P arkinson's disease: A hybrid PET/MR study using 18 F-FP-CIT. *Human Brain Mapping*, *37*(5), 1710–1721.

Choi, H., Jin, K. H., & Initiative, A. s. D. N. (2018). Predicting cognitive decline with deep learning of brain metabolism and amyloid imaging. *Behavioural Brain Research*, *344*, 103–109.

De Pablo-Fernandez, E., Lees, A. J., Holton, J. L., & Warner, T. T. (2019). Prognosis and Neuropathologic correlation of clinical subtypes of

Parkinson disease. *JAMA Neurology*, *76*, 470–479. https://doi.org/10.1001/jamaneurol.2018.4377

Erro, R., Picillo, M., Vitale, C., Palladino, R., Amboni, M., Moccia, M., … Barone, P. (2016). Clinical clusters and dopaminergic dysfunction in de-novo Parkinson disease. *Parkinsonism & Related Disorders*, *28*, 137–140. https://doi.org/10.1016/j.parkreldis.2016.04.026

Espay, A. J., Schwarzschild, M. A., Tanner, C. M., Fernandez, H. H., Simon, D. K., Leverenz, J. B., … Lang, A. E. (2017). Biomarker-driven phenotyping in Parkinson's disease: A translational missing link in disease-modifying clinical trials. *Movement Disorders*, *32*(3), 319–324. https://doi.org/10.1002/mds.26913

Faghri, F., Hashemi, S. H., Leonard, H., Scholz, S. W., Campbell, R. H., Nalls, M. A., & Singleton, A. B. (2018). Predicting onset, progression, and clinical subtypes of Parkinson disease using machine learning. *bioRxiv*, 338913. https://doi.org/10.1101/338913

Fereshtehnejad, S. M., Romenets, S. R., Anang, J. B., Latreille, V., Gagnon, J. F., & Postuma, R. B. (2015). New clinical subtypes of Parkinson disease and their longitudinal progression: A prospective cohort comparison with other phenotypes. *JAMA Neurology*, *72*(8), 863–873. https://doi.org/10.1001/jamaneurol.2015.0703

Filippi, L., Manni, C., Pierantozzi, M., Brusa, L., Danieli, R., Stanzione, P., & Schillaci, O. (2006). 123I-FP-CIT in progressive supranuclear palsy and in Parkinson's disease: A SPECT semiquantitative study. *Nuclear Medicine Communications*, *27*(4), 381–386. https://doi.org/10.1097/01.mnm.0000202858.45522.df

Foltynie, T., Brayne, C., & Barker, R. A. (2002). The heterogeneity of idiopathic Parkinson's disease. *Journal of Neurology*, *249*(2), 138–145.

Giladi, N., Kao, R., & Fahn, S. (1997). Freezing phenomenon in patients with parkinsonian syndromes. *Movement Disorders*, *12*(3), 302–305. https://doi.org/10.1002/mds.870120307

Gilman, S., Wenning, G., Low, P. A., Brooks, D., Mathias, C., Trojanowski, J., … Vidailhet, M. (2008). Second consensus statement on the diagnosis of multiple system atrophy. *Neurology*, *71*(9), 670–676. https://doi.org/10.1212/01.wnl.0000324625.00404.15

Hughes, A. J., Daniel, S. E., Kilford, L., & Lees, A. J. (1992). Accuracy of clinical diagnosis of idiopathic Parkinson's disease: A clinico-pathological study of 100 cases. *Journal of Neurology, Neurosurgery, and Psychiatry*, *55*(3), 181–184. https://doi.org/10.1136/jnnp.55.3.181

Hughes, A. J., Daniel, S. E., & Lees, A. J. (1993). The clinical features of Parkinson's disease in 100 histologically proven cases. *Advances in Neurology*, *60*, 595–599.

Jankovic, J. (2008). Parkinson's disease: Clinical features and diagnosis. *Journal of Neurology, Neurosurgery, and Psychiatry*, *79*(4), 368–376. https://doi.org/10.1136/jnnp.2007.131045

Kahraman, D., Eggers, C., Schicha, H., Timmermann, L., & Schmidt, M. (2012). Visual assessment of dopaminergic degeneration pattern in 123I-FP-CIT SPECT differentiates patients with atypical parkinsonian syndromes and idiopathic Parkinson's disease. *Journal of Neurology*, *259*(2), 251–260. https://doi.org/10.1007/s00415-011-6163-1

Kim, Y.-i., Im, H.-J., Paeng, J. C., Lee, J. S., Eo, J. S., Kim, D. H., … Lee, D. S. (2012). Validation of simple quantification methods for 18 F-FP-CIT PET using automatic delineation of volumes of interest based on statistical probabilistic anatomical mapping and isocontour margin setting. *Nuclear Medicine and Molecular Imaging*, *46*(4), 254–260.

Kordower, J. H., Olanow, C. W., Dodiya, H. B., Chu, Y., Beach, T. G., Adler, C. H., … Bartus, R. T. (2013). Disease duration and the integrity of the nigrostriatal system in Parkinson's disease. *Brain*, *136*(Pt 8), 2419–2431. https://doi.org/10.1093/brain/awt192

Lawton, M., Ben-Shlomo, Y., May, M. T., Baig, F., Barber, T. R., Klein, J. C., … Hu, M. T. M. (2018). Developing and validating Parkinson's disease subtypes and their motor and cognitive progression. *Journal of Neurology, Neurosurgery, and Psychiatry*, *89*(12), 1279–1287. https://doi.org/10.1136/jnnp-2018-318337

Lee, I., Kim, J. S., Park, J. Y., Byun, B. H., Park, S. Y., Choi, J. H., … Chi, D. Y. (2018). Head-to-head comparison of 18F-FP-CIT and 123I-FP-CIT for dopamine transporter imaging in patients with Parkinson's disease: A preliminary study. *Synapse*, *72*(7), e22032.

Litvan, I., Agid, Y., Calne, D., Campbell, G., Dubois, B., Duvoisin, R., … Zee, D. S. (1996). Clinical research criteria for the diagnosis of progressive supranuclear palsy (Steele-Richardson-Olszewski syndrome): Report of the NINDS-SPSP international workshop. *Neurology*, *47*(1), 1–9. https://doi.org/10.1212/wnl.47.1.1

Maaten, L. v. d., & Hinton, G. (2008). Visualizing data using t-SNE. *Journal of Machine Learning Research*, *9*(Nov), 2579–2605.

Marras, C., & Chaudhuri, K. R. (2016). Nonmotor features of Parkinson's disease subtypes. *Movement Disorders*, *31*(8), 1095–1102. https://doi.org/10.1002/mds.26510

Marras, C., & Lang, A. (2013). Parkinson's disease subtypes: Lost in translation? *Journal of Neurology, Neurosurgery, and Psychiatry*, *84*(4), 409–415. https://doi.org/10.1136/jnnp-2012-303455

Mestre, T. A., Eberly, S., Tanner, C., Grimes, D., Lang, A. E., Oakes, D., & Marras, C. (2018). Reproducibility of data-driven Parkinson's disease subtypes for clinical research. *Parkinsonism & Related Disorders*, *56*, 102–106. https://doi.org/10.1016/j.parkreldis.2018.07.009

Murphy, K. E., Karaconji, T., Hardman, C. D., & Halliday, G. M. (2008). Excessive dopamine neuron loss in progressive supranuclear palsy. *Movement Disorders*, *23*(4), 607–610. https://doi.org/10.1002/mds.21907

Nutt, J. G., Carter, J. H., & Sexton, G. J. (2004). The dopamine transporter: Importance in Parkinson's disease. *Annals of Neurology*, *55*(6), 766–773. https://doi.org/10.1002/ana.20089

Oh, M., Kim, J. S., Kim, J. Y., Shin, K. H., Park, S. H., Kim, H. O., … Lee, C. S. (2012). Subregional patterns of preferential striatal dopamine transporter loss differ in Parkinson disease, progressive supranuclear palsy, and multiple-system atrophy. *Journal of Nuclear Medicine*, *53*(3), 399–406. https://doi.org/10.2967/jnumed.111.095224

Postuma, R. B., Berg, D., Stern, M., Poewe, W., Olanow, C. W., Oertel, W., … Deuschl, G. (2015). MDS clinical diagnostic criteria for Parkinson's disease. *Movement Disorders*, *30*(12), 1591–1601. https://doi.org/10.1002/mds.26424

Saari, L., Kivinen, K., Gardberg, M., Joutsa, J., Noponen, T., & Kaasinen, V. (2017). Dopamine transporter imaging does not predict the number of nigral neurons in Parkinson disease. *Neurology*, *88*(15), 1461–1467. https://doi.org/10.1212/WNL.0000000000003810

Thenganatt, M. A., & Jankovic, J. (2014). Parkinson disease subtypes. *JAMA Neurology*, *71*(4), 499–504. https://doi.org/10.1001/jamaneurol.2013.6233

Titova, N., Padmakumar, C., Lewis, S. J. G., & Chaudhuri, K. R. (2017). Parkinson's: A syndrome rather than a disease? *Journal of Neural Transmission (Vienna)*, *124*(8), 907–914. https://doi.org/10.1007/s00702-016-1667-6

Tolosa, E., Wenning, G., & Poewe, W. (2006). The diagnosis of Parkinson's disease. *The Lancet Neurology*, *5*(1), 75–86.

van Rooden, S. M., Colas, F., Martinez-Martin, P., Visser, M., Verbaan, D., Marinus, J., … van Hilten, J. J. (2011). Clinical subtypes of Parkinson's disease. *Movement Disorders*, *26*(1), 51–58. https://doi.org/10.1002/mds.23346

SUPPORTING INFORMATION

Additional supporting information may be found online in the Supporting Information section at the end of this article.

How to cite this article: Suh M, Im JH, Choi H, Kim H-J, Cheon GJ, Jeon B. Unsupervised clustering of dopamine transporter PET imaging discovers heterogeneity of parkinsonism. *Hum Brain Mapp*. 2020;41:4744–4752. https://doi.org/10.1002/hbm.25155